

See discussions, stats, and author profiles for this publication at: <https://www.researchgate.net/publication/263982282>

Solubility, Density, Refractive Index, Viscosity, and Electrical Conductivity of Boric Acid + Lithium Sulfate + Water System at (293.15, 298.15, 303.15, 308.15 and 313.15) K

ARTICLE in JOURNAL OF CHEMICAL & ENGINEERING DATA · MAY 2013

Impact Factor: 2.04 · DOI: 10.1021/je400086a

CITATIONS

3

READS

179

4 AUTHORS, INCLUDING:



Wilson Alavia

16 PUBLICATIONS 6 CITATIONS

SEE PROFILE



Teófilo A. Graber

Universidad de Antofagasta, Chile

60 PUBLICATIONS 480 CITATIONS

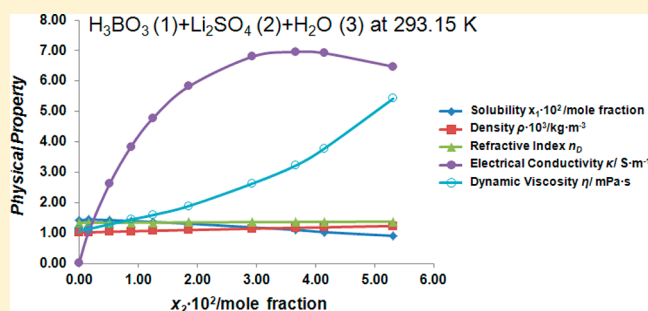
SEE PROFILE

Solubility, Density, Refractive Index, Viscosity, and Electrical Conductivity of Boric Acid + Lithium Sulfate + Water System at (293.15, 298.15, 303.15, 308.15 and 313.15) K

Wilson Alavia, Jorge A. Lovera, Brenda A. Cortez, and Teófilo A. Graber*

CICITEM, Departamento de Ingeniería Química, Universidad de Antofagasta, Avenue Universidad de Antofagasta 02800, Antofagasta, Chile

ABSTRACT: The solubility, density, refractive index, viscosity and electrical conductivity for aqueous solutions of Li_2SO_4 from (0 to 3.1472) $\text{mol}\cdot\text{kg}^{-1}\text{H}_2\text{O}$, saturated in H_3BO_3 , over the temperature range from (293.15 to 313.15) K have been determined. These physical properties were represented by equations as functions of temperature and Li_2SO_4 concentration. This information is useful for evaluating the physical properties of aqueous solutions saturated in H_3BO_3 in the range of concentrations of Li_2SO_4 and temperatures studied.



INTRODUCTION

Boric acid is a weak inorganic acid that has many applications, such as, antiseptic agent, flame retardant, and food preservative.¹ It is useful in preparing synthetic organic borate salts and other boron compounds.² As well, it is used as a chemical shim in pressurized water reactors in nuclear power plants.³ This acid is produced industrially by crystallization from brines or boron (3+) minerals.⁴ Brines are aqueous solutions from salt lakes that contain B^{3+} , Na^+ , K^+ , Li^+ , Mg^{2+} , Cl^- , and SO_4^{2-} species. The main boron (3+) minerals are boronatrocaltite, sodium tetraborate decahydrate, and hydrated calcium borate. The brines and boron (3+) mineral deposits in Chile are located in the northern region with the Salar de Atacama being the main source for boric acid production due to the high content of boron (3+) species in its brines.⁵

The boric acid production from brines starts with concentrating the brine by solar evaporation in ponds. In the first one NaCl is crystallized. The residual brine saturated in K^+ and SO_4^{2-} ions is sent to a second group of evaporation ponds, there NaCl,⁶ KCl, and some $\text{K}_2\text{SO}_4\cdot\text{MgSO}_4\cdot 6\text{H}_2\text{O}$ is crystallized. In the third group of ponds $\text{MgSO}_4\cdot\text{KCl}\cdot 3\text{H}_2\text{O}$, $\text{K}_2\text{SO}_4\cdot\text{MgSO}_4\cdot 6\text{H}_2\text{O}$, LiKSO_4 , KCl, and $\text{KMgCl}_3\cdot 6\text{H}_2\text{O}$ crystallizes. These salts are harvested from the ponds to be further processed. The final brine is used to produce boric acid by adding sulfuric acid. During this step, Li_2SO_4 could crystallize as $\text{Li}_2\text{SO}_4\cdot\text{H}_2\text{O}$ due to a salting out effect. Thus it is necessary to leach the crystals obtained before sending them to the drying stage.⁷ The impact of this impurity concentration in the crystallization yield and purity of the boric acid is evaluated, if its solubility in aqueous solution of lithium sulfate and the physical properties of its saturated solutions are known. As well that information is useful for the design and optimization of boric acid crystallization from brines.⁸

Because the effect of the physical properties of lithium sulfate in the boric acid production is important, we report in this contribution the solubility, density, refractive index, viscosity, and electrical conductivity for aqueous solutions of lithium sulfate saturated in boric acid at temperatures from (293.15 to 313.15) K, and Li_2SO_4 concentrations ranging from (0 to 3.1472) $\text{mol}\cdot\text{kg}^{-1}\text{H}_2\text{O}$.

In the literature physical properties data of aqueous solutions of sulfate salts that contain boron (3+) compounds are scarce. Linke and Seidell⁹ reported the solubility of H_3BO_3 in water at the temperature range from (273.15 to 454.15) K. As well they collected the solubility of H_3BO_3 in aqueous solutions of NaCl, KCl, LiCl at (285.15, 291.00, and 297.00) K, RbCl and CsCl at 291.15 K, BaCl_2 , MgCl_2 , and MgCl_2 at 291.00 K, and Na_2SO_4 at (293.65, 296.65, 298.15, 301.65, 308.15, and 348.15) K. Kolthoff¹⁰ presented solubility of H_3BO_3 in aqueous solutions of NaCl, KCl, LiCl, K_2SO_4 , at 293.15 K and Na_2SO_4 at 291.15 K. Chanson and Millero¹¹ determined the solubility of H_3BO_3 in electrolyte solutions (LiCl, NaCl, KCl, RbCl, and CsCl) as a function of the ionic strength at 298.15 K. Di Giacomo et al.^{8,12} measured the solubility of H_3BO_3 in aqueous solutions of NaCl, KCl, NaCl+KCl, K_2SO_4 , Na_2SO_4 , and $\text{K}_2\text{SO}_4+\text{Na}_2\text{SO}_4$ for a large range of concentrations at temperatures from (303.21 to 373.58) K. Novotny and Söhnel¹³ developed a correlation to estimate the densities of aqueous solutions of several inorganic substances including H_3BO_3 as a function of concentration and temperature. Galleguillos et al.¹⁴ measured experimental data of density and refractive index of aqueous solutions of H_3BO_3 and KCl at (293.15, 298.15 and 303.15) K. In a later work Galleguillos et al.⁶ reported the density of ternary aqueous

Received: January 25, 2013

Accepted: May 20, 2013

systems that contain H_3BO_3 with different electrolytes (NaCl , K_2SO_4 , and Na_2SO_4) at (298.15, 303.15 and 308.15) K.

■ EXPERIMENTAL SECTION

Materials. The chemical compounds used and their characteristics are described in Table 1. To remove the

Table 1. Detailed Description of Reagents Used

chemical name	source	mass fraction purity	purification method
boric acid	Loba Chemie	0.995	none
lithium sulfate monohydrated	Merck	0.990	none
(2R,3R,4R,5R)-hexan-1,2,3,4,5,6-hexol	Merck	0.990	none

humidity of the boric acid and the water molecule of lithium sulfate monohydrate, the compounds were dried in an oven at (333.15 and 393.15) K respectively for 24 h. Double distilled and deionized water (electrical conductivity of $0.0054 \mu\text{S}\cdot\text{cm}^{-1}$) were used in all procedures.

Apparatus and Procedures. Solution Preparation. Aqueous solutions saturated in boric acid were prepared for every temperature studied, based on the solubility data reported by Linke and Seidell.⁹ Boric acid and deionized water were massed and the resulting solution stirred to equilibrium. To prepare the ternary solutions, lithium sulfate monohydrate, a saturated solution in boric acid, and an excess of boric acid to ensure saturation in it were massed. An analytical balance with a precision of $\pm 0.0001\text{g}$ (Denver Instrument Co., model AA-200) was used to mass the reagents. The solutions prepared were kept under agitation at constant temperature for 96 h (equilibrium time) in a phase equilibrium unit which is composed by a rotatory basket located inside a thermostatically controlled water bath. Ten concentration levels of lithium sulfate were studied at temperatures ranging from (293.15 to 313.15) K. For every concentration, two solutions were prepared to ensure repeatability. The lithium sulfate concentrations prepared ranged from (0 to $3.1472 \text{ mol}\cdot\text{kg}^{-1} \text{H}_2\text{O}$).

To determine the equilibrium time, aqueous solutions of lithium sulfate of $1.7002 \text{ mol}\cdot\text{kg}^{-1} \text{H}_2\text{O}$, saturated in boric acid, were prepared and agitated at 303.15 K, using the phase equilibrium unit. Every 24 h a different solution was removed and its density was measured. That procedure was repeated until the density is constant, which indicates the solution has reached the thermodynamic equilibrium. The agitation time needed for the solutions to achieve that state is the equilibrium time.

Physical Properties Measurement. After equilibrium was reached the solutions were left settling for 12 h to improve the solid–liquid separation. For every solution a sample of 7 mL of liquid was removed, using a syringe filter ($0.45 \mu\text{m}$ pore size), and diluted to 250 mL, for its chemical analysis in Li^+ by SM3111B- atomic absorption,¹⁵ SO_4^{2-} by SM 4500-SO4-D¹⁵ and, H_3BO_3 by complexation with (2R,3R,4R,5R)-hexan-1,2,3,4,5,6-hexol and titration by NaOH of concentration $0.1004 \text{ mol}\cdot\text{kg}^{-1} \text{H}_2\text{O}$. The composition of the residual wet solid phase was analyzed for Li^+ , SO_4^{2-} , and H_3BO_3 by the methods mentioned above, to settle the solid in equilibrium with the saturated solution. The nature of this solid was determined by XRD when necessary. The accuracy and reproducibility of solution chemical composition measurements were better than (0.0004 and 0.00074) mole fraction,

respectively. The reproducibility of the measured data was determined compared to the H_3BO_3 solubility data from Linke and Seidell.⁹

To measure the other physical properties of the solutions a proper amount of sample was removed from every solution using a syringe filter ($0.45 \mu\text{m}$ pore size).

Density was measured with a vibrating tube densimeter (Mettler Toledo, model DE50). It has a precision of $0.05 \text{ kg}\cdot\text{m}^{-3}$ and reproducibility better than $\pm 1 \text{ kg}\cdot\text{m}^{-3}$. The density was measured in triplicate per sample at each mentioned temperature. The apparatus was calibrated previously, using distilled deionized water as a reference substance, before measuring for every temperature. The densimeter has a temperature control ($\pm 0.1 \text{ K}$). The time needed to reach temperature stability was 600 s. In the measuring cell about 2 mL of solution were introduced; the solution was not allowed to crystallize inside the cell.

Refractive index was measured with a refractometer (Mettler Toledo, model RE40) with a precision and reproducibility of ± 0.0001 . These values are measured at the yellow doublet sodium D-line, with $\lambda = 589 \text{ nm}$. Two drops of the sample were deposited on the prism of the instrument, using an airtight hypodermic syringe. Three measurements were made for each sample. After measurement, the solution was suctioned from the prism by a cleaning syringe; the prism was rinsed with distilled water and dried with tissue paper.

The kinematic viscosity was measured in triplicate for every solution with an automatic laser viscosimeter system (Schott-Gerate AVS 310). It measures the transit time of a liquid between two points in a capillary with a precision of $\pm 0.1 \text{ s}$. Two calibrated Micro-Ostwald capillaries with instrument constants, K , (0.01132 and 0.01111) $\text{mm}^2\cdot\text{s}^{-2}$, respectively, were used. Their calibration was made using four cannon-certified viscosity standards (N1.0 (b), N2, S3 (a), and N4) to include the whole range of dynamic viscosity measurements. The measurements ranged from $5.2 \text{ mPa}\cdot\text{s}$ to $0.70 \text{ mPa}\cdot\text{s}$ at (293.15 to 313.15) K. To measure the viscosity, 2 mL of solution was poured into the capillary and it was immersed inside a transparent thermostatic bath (Schott-Gerate CT 52) that had a temperature precision of $\pm 0.05 \text{ K}$. Dynamic viscosity data for every solution was determined using its kinematic viscosity and density measured.

Electrical conductivity was measured in triplicate for every solution using a conductivimeter (Orion, model 19700-27) with a precision $< 0.5 \%$ and reproducibility of $\pm 0.7 \%$. It was calibrated using a standard KCl solution, fixing a cell constant of 0.604 cm^{-1} . The conductivimeter cell was introduced in the flask containing the solution, and the instrument readings were recorded. After every measurement the flask was rinsed with distilled water and dried with tissue paper. To keep the temperature constant for the measurements, a digital immersion circulator (Thermo Haake, DC3) of (298.15 to 423.15) K temperature range and a refrigerated water bath vessel (Thermo Haake, V) of 15 L capacity and refrigerant R134A for refrigeration down to 268.15 K were used.

■ RESULTS AND DISCUSSION

Table 2 is presents the solubility x_1 , density ρ , refractive index n_D , dynamic viscosity η , and electrical conductivity κ of saturated solutions for $\text{H}_3\text{BO}_3 + \text{Li}_2\text{SO}_4 + \text{H}_2\text{O}$ as a function of mole fraction of Li_2SO_4 , x_2 , at temperatures T of (293.15, 298.15, 303.15, 308.15, and 313.15) K. The standard uncertainty, $u(x_2)$, is $0.0002 \text{ mol fraction}$. It was determined

Table 2. Solubility x_1 , Density ρ , Refractive Index n_D , Viscosity η , and Electrical Conductivity κ of Aqueous Solutions of Li_2SO_4 Saturated in H_3BO_3 for different Li_2SO_4 Mole Fraction, x_2 , at (293.15, 298.15, 303.15, 308.15 and 313.15) K^a

$x_2 \cdot 10^2$	$x_1 \cdot 10^2$	solid phase	$\rho/\text{kg}\cdot\text{m}^{-3}$	n_D	$\eta/\text{mPa}\cdot\text{s}$	$\kappa/\text{S}\cdot\text{m}^{-1}$
$T = 293.15 \text{ K}$						
0.00	1.41	H_3BO_3	1015.5	1.3363	1.0994	0.008
0.17	1.44	H_3BO_3	1023.9	1.3379	1.1420	1.074
0.52	1.42	H_3BO_3	1041.0	1.3413	1.2885	2.629
0.88	1.40	H_3BO_3	1058.2	1.3447	1.4436	3.835
1.25	1.36	H_3BO_3	1075.3	1.3479	1.5926	4.780
1.86	1.31	H_3BO_3	1100.8	1.3527	1.8908	5.825
2.94	1.19	H_3BO_3	1145.0	1.3608	2.6302	6.805
3.66	1.10	H_3BO_3	1172.7	1.3658	3.2163	6.957
4.15	1.03	H_3BO_3	1190.1	1.3688	3.7714	6.919
5.32	0.91	$\text{H}_3\text{BO}_3 + \text{Li}_2\text{SO}_4$	1230.7	1.3757	5.4207	6.477
$T = 298.15 \text{ K}$						
0.00	1.67	H_3BO_3	1016.5	1.3360	0.9765	0.010
0.17	1.65	H_3BO_3	1024.9	1.3377	1.0377	1.189
0.53	1.63	H_3BO_3	1041.5	1.3410	1.1327	2.880
0.90	1.60	H_3BO_3	1058.7	1.3443	1.2685	4.210
1.25	1.56	H_3BO_3	1075.4	1.3475	1.4313	5.242
1.86	1.51	H_3BO_3	1101.4	1.3524	1.6646	6.420
2.92	1.37	H_3BO_3	1145.1	1.3604	2.3062	7.490
3.66	1.27	H_3BO_3	1172.1	1.3653	2.8493	7.710
4.11	1.21	H_3BO_3	1187.9	1.3680	3.2626	7.700
5.25	1.05	$\text{H}_3\text{BO}_3 + \text{Li}_2\text{SO}_4$	1229.8	1.3753	4.7047	7.284
$T = 303.15 \text{ K}$						
0.00	1.95	H_3BO_3	1017.5	1.3359	0.8886	0.011
0.17	1.92	H_3BO_3	1026.0	1.3376	0.9445	1.179
0.53	1.89	H_3BO_3	1043.3	1.3410	1.0316	2.852
0.89	1.85	H_3BO_3	1059.4	1.3442	1.1590	4.115
1.26	1.80	H_3BO_3	1077.1	1.3476	1.3191	5.167
1.91	1.74	H_3BO_3	1103.4	1.3519	1.5355	7.067
3.04	1.59	H_3BO_3	1146.6	1.3599	2.1415	8.222
3.67	1.45	H_3BO_3	1175.6	1.3654	2.6806	8.455
4.11	1.38	H_3BO_3	1193.7	1.3687	3.0636	8.384
5.06	1.23	$\text{H}_3\text{BO}_3 + \text{Li}_2\text{SO}_4$	1230.1	1.3749	4.1852	7.999
$T = 308.15 \text{ K}$						
0.00	2.34	H_3BO_3	1018.8	1.3358	0.8048	0.027
0.18	2.19	H_3BO_3	1027.0	1.3375	0.8518	1.408
0.52	2.14	H_3BO_3	1044.4	1.3407	0.9573	3.440
0.89	2.13	H_3BO_3	1061.2	1.3440	1.0627	5.009
1.27	2.11	H_3BO_3	1078.4	1.3472	1.1913	6.275
1.86	1.92	H_3BO_3	1104.4	1.3522	1.3862	7.677
3.06	1.84	H_3BO_3	1148.7	1.3604	1.9321	9.014
3.81	1.70	H_3BO_3	1179.2	1.3652	2.3449	9.270
4.22	1.57	H_3BO_3	1194.5	1.3683	2.6724	9.235
5.10	1.44	$\text{H}_3\text{BO}_3 + \text{Li}_2\text{SO}_4$	1227.0	1.3739	3.6191	8.945
$T = 313.15 \text{ K}$						
0.00	2.49	H_3BO_3	1019.5	1.3354	0.7524	0.018
0.17	2.46	H_3BO_3	1028.0	1.3371	0.7996	1.537
0.53	2.46	H_3BO_3	1045.0	1.3406	0.8974	3.710
0.89	2.38	H_3BO_3	1061.7	1.3438	0.9814	5.409
1.27	2.31	H_3BO_3	1079.0	1.3472	1.1100	6.772
1.82	2.25	H_3BO_3	1104.5	1.3519	1.2960	8.222
2.92	2.06	H_3BO_3	1149.8	1.3602	1.7884	9.707
3.61	1.91	H_3BO_3	1176.7	1.3651	2.1853	10.008
4.19	1.82	H_3BO_3	1195.8	1.3684	2.5527	10.014
4.91	1.66	$\text{H}_3\text{BO}_3 + \text{Li}_2\text{SO}_4$	1224.7	1.3733	3.2413	9.743

^aStandard uncertainties u are $u(T) = 0.06 \text{ K}$, $u(x_1) = 0.0001$, $u(x_2) = 0.0002$, and the combined expanded uncertainties U_c at 0.95 level of confidence and $k = 2$ are $U_c(\rho) = 0.4 \text{ kg}\cdot\text{m}^{-3}$, $U_c(n_D) = 0.0005$, $U_c(\eta) = 0.0194 \text{ mPa}\cdot\text{s}$ and $U_c(\kappa) = 0.303 \text{ S}\cdot\text{m}^{-1}$.

following the guidelines for evaluating the uncertainty by NIST.¹⁶ The accuracy of the measured data was determined as compared to the H_3BO_3 solubility data from Seidell and Linke⁹ and its density, estimated using the correlation given by Novotný and Söhnel.¹³ The reproducibility for solubility is better than 0.0007 mol fraction and for density better than $0.6 \text{ kg}\cdot\text{m}^{-3}$. It was not possible to determine the accuracy for the other properties because there is no reported data in literature for aqueous solutions saturated in H_3BO_3 and the system studied. The standard uncertainty for the temperature, $u(T)$, is 0.06 K.

The data of boric acid determined is reported with repeatability better than 0.0017 and standard uncertainty, $u(x_1) = 0.0001$ mol fraction. By applying the residual wet method,¹⁷ it was determined that the solid phase in equilibrium with the saturated solution is H_3BO_3 , but for the last concentration of lithium sulfate, at every temperature, the solid phase is $\text{H}_3\text{BO}_3 + \text{Li}_2\text{SO}_4\cdot\text{H}_2\text{O}$ (eutectic point) as it was confirmed analyzing that point by XRD.

The measured data were illustrated in Figure 1. It shows that boric acid solubility decreases with increases of mole fraction of

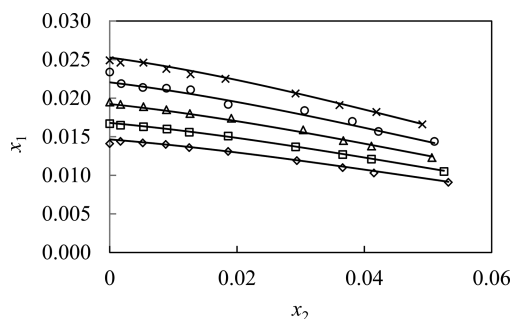


Figure 1. Solubility x_1 of boric acid as a function of lithium sulfate mole fraction, x_2 : this study (\diamond , $T = 293.15 \text{ K}$; \square , $T = 298.15 \text{ K}$, Δ , $T = 303.15 \text{ K}$, \circ , $T = 308.15 \text{ K}$, \times , $T = 313.15 \text{ K}$); —, calculated from eq 1.

lithium sulfate at constant temperature, due to a salting out effect, given by the structure making characteristic of Li^+ ion.¹¹ The temperature effect was the same as the effect in aqueous solutions of boric acid,⁹ increasing solubility with increases of temperature.

The values of solubility of H_3BO_3 measured in aqueous solutions of Li_2SO_4 are smaller than in H_2O at the same temperature.⁹ The solubility values measured are similar to the ones in $\text{LiCl} + \text{H}_2\text{O}$.¹¹ In both cases the solubility decreases as salt concentration increases. Mainly it can be assumed as the effect of the presence of Li^+ ions. This behavior is inverse to that presented in aqueous solutions of NaCl ,⁸ KCl ,⁸ $\text{NaCl} + \text{KCl}$,⁸ K_2SO_4 ,^{10,12} and Na_2SO_4 ,¹² where the solubility of the H_3BO_3 increases with salt concentration increasing.^{10,11,12}

To describe the experimental data, it was fitted to a curve according to the following equation:

$$\ln x_1(x_2, T)/\text{mole fraction} = A_0(x_2) + B_0(x_2)T/K \quad (1)$$

with

$$A_0(x_2) = \sum_{i=0} a_{0i}(x_2/\text{mole fraction})^i \quad (2)$$

$$B_0(x_2) = \sum_{i=0} a_{0i}(x_2/\text{mole fraction})^i \quad (3)$$

where T is the absolute temperature, $i = 0, 1, 2, \dots$, etc. The coefficients a_{0i} and b_{0i} are constants and were estimated using the least-squares method.

Four constants (a_{00} , a_{01} , a_{02} , and b_{00}) of the model were necessary to describe the experimental data. The values obtained for the constants are in Table 3. The curve families of tendency of the logarithm of the solubility are parabolas. The 99.43 % of the variance of the experimental data are explained by the model as was proven by the coefficient of multiple determination $R^2 = 0.9943$. The standard error of estimate is given by

$$SD = \sqrt{\frac{\sum_{i=1}^n (y_i - \hat{y}_i)^2}{n - p}} \quad (4)$$

where y , \hat{y} , n , and p represent the observed value, predicted value, number of data points, and parameters, respectively. The calculated value is 0.0003 mol fraction of H_3BO_3 and the maximum residual between experimental and predicted values is 0.0014 mol fraction. Equation 4 is applied to calculate the fit estimating error for the rest of correlations reported in this study.

Density values were measured with a repeatability better than $1.8 \text{ kg}\cdot\text{m}^{-3}$. Figure 2 presents the experimental values as function of the lithium concentration for every temperature studied. It can be observed that density depends on the sulfate salt concentration, increasing its value as salt concentration increases. With respect to the temperature effect, density typically decreases with temperature increases for aqueous solutions, but it does not in the presence of lithium sulfate. This can be explained due to the fact that the solubility of boric acid increases with temperature at the same concentration of lithium sulfate, thus increasing the total solid concentration.

The density values measured were compared to the ones for aqueous solutions of this salt, at the same temperatures and concentrations, reported by Carton et al.¹⁸ It was found that the density measured has the same behavior with respect to the salt concentration and value as density of this salt in water; it is shown in Figure 2. This fact can be explained due to the fact that the lithium sulfate decreases the solubility of boric acid, its contribution being small to the density value.

Refractive index data were obtained having a repeatability less than 0.0004. The refractive index depends on lithium sulfate concentration, increasing as salt concentration increases, but it does not depend on temperature. This behavior is similar to that shown by the density and it can be assumed that the total solid concentration increases with temperature.

Because the density and refractive index present similar conducts, they are described by the same relation with sulfate concentration. That function is expressed mathematically by

$$Y_j(x_2) = \sum_{i=0} a_{ij}(x_2/\text{mole fraction})^i \quad (5)$$

where Y_j represents the density or the refractive index (it means, $j = 1$ or 2 , respectively); the i subscript changes as before. The coefficients a_{ij} are parameters of the model.

The density data were represented well by the model using two parameters (a_{10} and a_{11}), verifying that the influence of temperature is negligible as compared to that of the salt concentration. The estimated error is $3.9 \text{ kg}\cdot\text{m}^{-3}$, and the maximum residual is $7.7 \text{ kg}\cdot\text{m}^{-3}$. The combined expanded uncertainty, U_c , was determined following the guidelines for evaluating the uncertainty by NIST.¹⁶ The value found, at 0.95

Table 3. Coefficients of eqs 1–9^b

property	a_{10}	a_{11}	a_{12}	b_{10}	b_{11}	b_{12}	b_{13}	R^2	SD
x_1	-12.218 ± 0.236	-4.5364 ± 1.1983	-80.777 ± 25.425	0.027270 ± 0.000773				0.9943	0.0003
ρ	1022.0 ± 1.7	4115.8 ± 63.6						0.9972	3.9
n_D	1.3371 ± 0.0004	0.75684 ± 0.01534						0.9951	0.0009
η	6.9865 ± 0.3461		53.564 ± 32.870	-0.023367 ± 0.001169	0.088997 ± 0.006832			0.9974	0.0587
κ	-9.0345 ± 3.8991	-756.59 ± 146.52		0.030404 ± 0.012870	4.4738 ± 0.4986	-46.733 ± 4.317	354.62 ± 55.37	0.9962	0.204

^bThe confidence intervals for all the parameters are reported at 0.95 level of confidence.

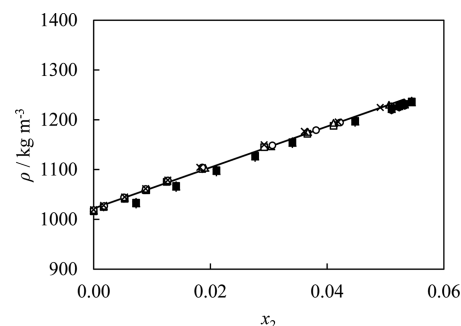


Figure 2. Density ρ of aqueous solutions of lithium sulfate saturated in boric acid as a function of lithium sulfate mole fraction, x_2 : this study (\diamond , $T = 293.15$ K; \square , $T = 298.15$ K, Δ , $T = 303.15$ K, \circ , $T = 308.15$ K, \times , $T = 313.15$ K); $-$, calculated from eq 5. Reference 18 (\blacklozenge , $T = 293.15$ K; \blacksquare , $T = 298.15$ K, \blacktriangle , $T = 303.15$ K, \bullet , $T = 308.15$ K, $+$, $T = 313.15$ K).

level of confidence and $k = 2$, is $U_c(\rho) = 0.4 \text{ kg} \cdot \text{m}^{-3}$. The model describes 99.72 % of the variability of the experimental data ($R^2 = 0.9972$). The values of the parameters obtained are given in Table 3 and the calculated values are illustrated in Figure 2.

The refractive index of the ternary solution was fitted to the empirical model using a_{20} and a_{21} parameters, 99.51 % being the variability of the refractive index data described by the model ($R^2 = 0.9951$), with an estimated error of 0.0009 and maximum residual of 0.0016. The combined expanded uncertainty, at the 0.95 level of confidence and $k = 2$, is $U_c(n_D) = 0.0005$. The corresponding values to the model are shown in Table 3 and the calculated values are illustrated in Figure 3.

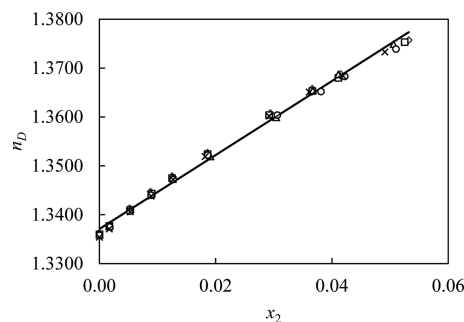


Figure 3. Refractive Index n_D of aqueous solutions of lithium sulfate saturated in boric acid as a function of lithium sulfate mole fraction, x_2 : this study (\diamond , $T = 293.15$ K; \square , $T = 298.15$ K, Δ , $T = 303.15$ K, \circ , $T = 308.15$ K, \times , $T = 313.15$ K); $-$, calculated from eq 5.

Dynamic viscosity data were measured with a repeatability of 0.0148 mPa·s. It was observed that viscosity increases as salt concentration increases at constant temperature, for the structure maker effect of Li^+ ion which leads to greater packing of the solution. The viscosity decreases as the temperature value increases, because the solution packing decreases as the temperature rises. Therefore the following equation was chosen to describe these data:

$$\ln \eta(x_2, T) / \text{mPa} \cdot \text{s} = A_3(x_2) + B_3(x_2)T/K \quad (6)$$

$$A_3(x_2) = \sum_{i=0} a_{ij}(x_2/\text{mole fraction})^i \quad (7)$$

$$B_3(x_2) = \sum_{i=0} b_{ij}(x_2/\text{mole fraction})^i \quad (8)$$

A_3 and B_3 represent potential series of x_2 .

The experimental data are represented well by the model, using four parameters of the potential series (a_{30} , a_{32} , b_{30} , and b_{31}), with an estimated error of 0.0587 mPa·s and maximum residual of 0.1091 mPa·s. The combined expanded uncertainty, at 0.95 level of confidence and $k = 2$, is $U_c(\eta) = 0.0194$ mPa·s; 99.74 % of the variability of the viscosity data are described by this model ($R^2 = 0.9974$). The parameters values and the goodness of fit are given in Table 3. The correlation is positive for all temperatures studied as seen in Figure 4.

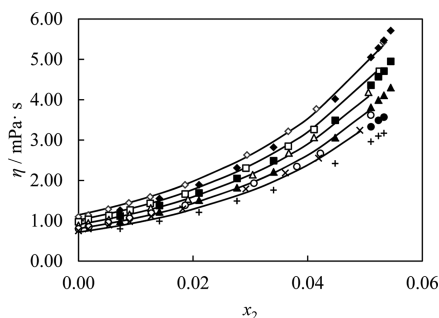


Figure 4. Viscosity η of aqueous solutions of lithium sulfate saturated in boric acid as a function of lithium sulfate mole fraction, x_2 : this study (\diamond , $T = 293.15$ K; \square , $T = 298.15$ K; Δ , $T = 303.15$ K; \circ , $T = 308.15$ K; \times , $T = 313.15$ K); —, calculated from eq 6. Reference 18 (\blacklozenge , $T = 293.15$ K; \blacksquare , $T = 298.15$ K; \blacktriangle , $T = 303.15$ K; \bullet , $T = 308.15$ K; $+$, $T = 313.15$ K).

The viscosity values measured were compared to the viscosity of solutions of this salt in water, at the same temperatures and concentrations, reported by Carton et al.¹⁸ It was found that the viscosities measured have the same behavior with respect to the salt concentration and higher value than viscosities of this salt in water, as can be observed in Figure 4. It can be explained for a decrease in the solubility of boric acid by lithium sulfate; the acid contribution to the viscosity value being small.

Electrical conductivity data were reported with a repeatability better than $1.01 \text{ S}\cdot\text{m}^{-1}$. The conductivity depends on lithium sulfate concentration, increasing with salt concentration increases until reaching a maximum value, after which it decreases. The presence of that maximum may be explained by the system reaching the maximum ionic mobility at the salt concentrations shown in Figure 5, a further increase of concentration results in the reduction of the ionic mobility by complex species formation. Temperature affects the conductivity as well, increasing its value for the promotion of the ionic mobility of SO_4^{2-} and Li^+ ions because of the viscosity decreases.

Thus a regression curve for electrical conductivity (κ) function of mole fraction of lithium sulfate (x_2) and temperature (T) was chosen. It is expressed by

$$\kappa(x_2, T)/\text{S}\cdot\text{m}^{-1} = A_4(x_2) + B_4(x_2)\frac{1}{T/K} \quad (9)$$

where A_4 and B_4 depend on x_2 exclusively, and it has the same functional behavior as eqs 7 and 8, respectively. The parameters a_{40} , a_{41} , b_{40} , b_{41} , b_{42} , and b_{43} were needed to describe the data with the model. The parameter values and the goodness of fit

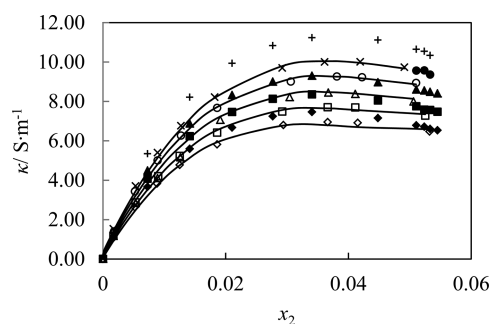


Figure 5. Electrical conductivity κ of aqueous solutions of lithium sulfate saturated in boric acid as a function of lithium sulfate mole fraction, x_2 : this study (\diamond , $T = 293.15$ K; \square , $T = 298.15$ K; Δ , $T = 303.15$ K; \circ , $T = 308.15$ K; \times , $T = 313.15$ K); —, calculated from eq 9. Reference 18 (\blacklozenge , $T = 293.15$ K; \blacksquare , $T = 298.15$ K; \blacktriangle , $T = 303.15$ K; \bullet , $T = 308.15$ K; $+$, $T = 313.15$ K).

are given in Table 3. The conductivity data were fitted well ($R^2 = 0.9962$) as can be seen in Figure 5. The estimating error of ionic conductivity calculated is $0.204 \text{ S}\cdot\text{m}^{-1}$ and the maximum residual is $0.275 \text{ S}\cdot\text{m}^{-1}$. The combined expanded uncertainty, at 0.95 level of confidence and $k = 2$, is $U_c(\kappa) = 0.303 \text{ S}\cdot\text{m}^{-1}$.

The electrical conductivity measured values were compared to the electrical conductivity of solutions of this salt in water at the same temperatures and concentrations reported by Carton et al.¹⁸ It was observed that viscosities measured have the same behavior respect to the salt concentration and smaller values than viscosities of this salt in water as shown in Figure 5. It can be attributed to the weak dissociation of boric acid, its contribution to the electrical conductivity value being negligible compared with the lithium sulfate one and the fact that ionic mobilities of SO_4^{2-} and Li^+ ions are lower than that corresponding to an aqueous solution of Li_2SO_4 , because of the higher viscosity of the solutions studied.

CONCLUSIONS

This work provides reliable data of solubility of boric acid, density, refractive index, dynamic viscosity, and electrical conductivity data of aqueous solutions of lithium sulfate saturated in boric acid at temperature ranges from (293.15 to 313.15) K. The experimental data were correlated by empirical equations, obtaining a good enough fit to be useful for evaluating the physical properties of aqueous solutions saturated in boric acid, in the range studied of concentrations of lithium sulfate and temperatures.

AUTHOR INFORMATION

Corresponding Author

*E-mail: tgrabert@uantof.cl. Tel.: 56 55 637313. Address: Av. Angamos 601. Antofagasta, Chile.

Funding

The authors are grateful for the funding provided by CONICYT through the FONDECYT Project No. 1120192 and CICITEM Project R04I1001. Wilson Alavia acknowledges the Ministerio de Educación de Chile, through Project Mecespun_ANT0709 and Universidad de Antofagasta for the support to doctoral studies.

Notes

The authors declare no competing financial interest.

■ REFERENCES

- (1) Elango, M.; Subramanian, V.; Rahalkar, A. P.; Gadre, S. R.; Sathyamurthy, N. Structure, energetics, and reactivity of boric acid nanotubes: A molecular tailoring approach. *J. Phys. Chem. A* **2008**, *112*, 7699–7704.
- (2) Ekmekyapar, A.; Demirkıran, N.; Künkül, A. Dissolution kinetics of ulexite in acetic acid solutions. *Chem. Eng. Res. Des.* **2008**, *86*, 1011–1016.
- (3) Malik, J. I.; Mirza, N. M.; Mirza, S. M. Time-dependent corrosion product activity in a typical PWR due to changes in coolant chemistry for long-term fuel cycles. *Prog. Nucl. Energy* **2012**, *58*, 100–107.
- (4) Mergen, A.; Demirhan, M. H.; Bilen, M. Processing of boric acid from borax by a wet chemical method. *Adv. Powder Technol.* **2003**, *14*, 279–293.
- (5) Chong, G.; Pueyo, J. J.; Demergasso, C. The borate deposits in Chile. *Andean Geol.* **2000**, *27*, 99–119.
- (6) Galleguillos, H. R.; Molina, M. A.; Graber, T. A.; Taboada, M. E.; Hernandez-Luis, F. Experimental determination of densities of aqueous electrolyte mixtures containing B(OH)(3) or Na₂B₄O₇ and their correlation with the Pitzer model. *Ind. Eng. Chem. Res.* **2006**, *45*, 6604–6613.
- (7) Pavlovic-Zuvic, P.; Parada-Frederick, N.; Vergara-Edwards, L. In Sixth International Symposium on Salt; Salt Institute: Alexandria, WV, 1983; Vol. II, pp 381, 386, 387.
- (8) Digiaco, G.; Brandani, P.; Brandani, V.; Delre, G. Solubility of boric-acid in aqueous-solutions of chloride salts. *Desalination* **1993**, *91*, 21–33.
- (9) Linke, W. F.; Seidell, A.; *Solubilities of Inorganic and Metal-Organic Compounds*, 4th ed.; Van Nostrand: Princeton, N.J., 1958.
- (10) Kolthoff, I. M. The influence of boric acid on the electrolytic dissociation of electrolytes. *Recl. Trav. Chim. Pays-Bas* **1926**, *45*, 394–399.
- (11) Chanson, M.; Millero, F. J. The solubility of boric acid in electrolyte solutions. *J. Solution Chem.* **2006**, *35*, 689–703.
- (12) Digiaco, G.; Brandani, P.; Brandani, V.; Delre, G. Solubility of boric-acid in aqueous-solutions of sulfate salts. *Desalination* **1992**, *89*, 185–202.
- (13) Novotny, P.; Sohnel, O. Densities of binary aqueous-solutions of 306 inorganic substances. *J. Chem. Eng. Data* **1988**, *33*, 49–55.
- (14) Galleguillos, H. R.; Flores, E. K.; Aguirre, C. E. Density and refractive index for boric acid plus potassium chloride plus water and disodium tetraborate plus potassium chloride plus water systems at (20, 25, and 30) degrees C. *J. Chem. Eng. Data* **2001**, *46*, 1632–1634.
- (15) Eaton, A. D.; Franson, M. A. H.; Associati, A. P. H.; Association, A. W. W.; Federation, W. E. *Standard Methods for the Examination of Water & Wastewater*; American Public Health Assn: Washington, DC, 2005.
- (16) Taylor, B. N.; Kuyatt, C. E. Guidelines for evaluating and expressing the uncertainty of NIST measurement results. *NIST Technical Note 1297*; NIST: Gaithersburg, MD, 1994; p 24
- (17) Castellan, G. W. *Physical Chemistry*; Addison-Wesley; Boston, MA, 1983.
- (18) Carton, A.; Sobron, F.; Bolado, S.; Gerboles, J. I. Density, Viscosity, and electrical conductivity of aqueous solutions of lithium sulfate. *J. Chem. Eng. Data* **1995**, *40*, 987–991.